SOILS AND FOUNDATIONS Vol. 48, No. 6, 755–770, Dec. 2008
Japanese Geotechnical Society

CPTU SIMPLIFIED STRESS-BASED MODEL FOR EVALUATING SOIL LIQUEFACTION POTENTIAL

C. HSEIN JUANG[i),ii)], CHIEN-HSUN CHEN[iii)] and PAUL W. MAYNE[iv)]

ABSTRACT

This paper presents a piezocone penetration test (CPTu) method for evaluating soil liquefaction potential covering a wider range of soil types than previous approaches and using simplified stress-based procedures. In the approach, the adjusted cyclic stress ratio is calculated with a recent formula created by Idriss and Boulanger, and the cyclic resistance ratio is determined as a function of both adjusted cone tip resistance (q_{t1N}) and soil behavior type index (I_c). The new method is established through artificial neural network learning of documented cases. One unique feature of this method is the inclusion of excess porewater pressure ratio (B_q) in the formulation of I_c as per Jefferies and Davies. The proposed method is shown to be more applicable to a *wider range* of soils, including geomaterials that were previously considered ''too clay-rich to liquefy.'' The ability of this method to delineate liquefied cases from non-liquefied cases is clearly depicted with 3-D and 2-D graphs. Case studies of selected ground failure sites in Adapazari using the proposed method yield results that agree well with field observations in the 1999 Kocaeli earthquake.

Key words: artificial neural network, case history, cone penetration test, cyclic resistance ratio, cyclic stress ratio, earthquake, liquefaction potential, model, piezocone (**IGC**: C3/E8)

INTRODUCTION

The simplified procedures for evaluating the liquefaction potential of a soil was created by Seed and Idriss (1971) in which the seismic loading required to initiate liquefaction was expressed as a cyclic stress ratio (CSR) and the soil resistance against liquefaction was measured by the energy-corrected blow count (N_{60}) from the standard penetration test (SPT). Using this general framework, many subsequent simplified models were later developed based on different *in situ* tests such as the cone penetration test (CPT), flat dilatometer test (DMT), Becker penetration test (BPT), and shear wave velocity (V_s) measurements. An excellent summary of the latest consensus versions of the SPT-, CPT-, and V_s-based models was documented by Youd et al. (2001). This paper focuses on the evaluation of liquefaction potential using CPT, in particular, the piezocone penetration test (CPTu) that obtains three readings with depth: cone tip resistance (q_t), sleeve friction (f_s), and penetration porewater pressures at the shoulder position (u_2).

Many investigators have contributed to the development of the CPT-based simplified models for liquefaction evaluation (e.g., Robertson and Campanella, 1985; Seed et al., 1986; Mitchell and Tseng, 1990; Stark and Olson, 1995; Suzuki et al., 1995; Olsen, 1997; Robertson and Wride, 1998; Juang et al., 2003; Moss et al., 2006). Among these CPT-based models or methods, that developed by Robertson and Wride (1998) and updated in Zhang et al. (2002) is arguably the most widely used. This method is a *deterministic* model, meaning that the soil and seismic parameters are treated as if they were not subject to random variations. Thusly, the assessment of liquefaction potential can be carried out with a calculated factor of safety (F_S), which is generally defined as the ratio of cyclic resistance ratio (CRR) over cyclic stress ratio (CSR). In a deterministic solution, the results are interpreted in a ''yes-or-no'' manner; the occurrence of liquefaction is ''predicted' if $F_S < 1$ whereas no liquefaction is predicted if $F_S > 1$.

CPT-based methods for liquefaction evaluation are attractive because of two important test characteristics: capability of continuous profiling and superior measurement repeatability over other *in situ* tests such as SPT (Shuttle and Cunning, 2007). The capability of continuous profiling is of particular advantage if the results of liquefaction potential evaluation at depths are to be integrated over the entire soil column into Liquefaction Potential Index (LPI), an index that is often used to characterize the potential for occurrence of damaging liquefaction in a geologic unit (Iwasaki et al., 1982; Toprak and Holzer, 2003; Li et al., 2006). During SPT

i) Professor, Department of Civil Engineering, Clemson University, Clemson, USA (hsein@clemson.edu).
ii) Chair Professor, Department of Civil Engineering, National Central University, Jungli, Taiwan.
iii) Research Assistant, Department of Civil Engineering, Clemson University, Clemson, USA.
iv) Professor, School of Civil and Environmental Engineering, Georgia Institute of Technology, Atlanta, USA.
The manuscript for this paper was received for review on May 9, 2008; approved on October 3, 2008.
Written discussions on this paper should be submitted before July 1, 2009 to the Japanese Geotechnical Society, 4-38-2, Sengoku, Bunkyo-ku, Tokyo 112-0011, Japan. Upon request the closing date may be extended one month.

and conventional shear wave methods (i.e., crosshole and downhole), common test intervals are at 1 to 1.5 m intervals, thereby perhaps missing weak layers in the profile.

Yet, in normal CPT practice, soil samples are not taken and examined, which can be a significant disadvantage compared to SPT. Furthermore, for the so-called ''clay-rich'' soils, defined by Robertson and Wride (1998) as those with soil behavior type index (I_c) greater than 2.6, the liquefaction potential must be confirmed by different means (such as the Chinese Criteria or those proposed by Bray and Sancio, 2006), although these soils are usually considered ''non-liquefiable.'' Because samples are not retrieved during CPT, the criteria such as those by Bray and Sancio (2006) are not readily applicable without additional data from nearby SPTs. This poses a challenge for the evaluation of liquefaction potential of silty and clayey soils using CPT and for the integration of the CPT-based evaluation into the framework of LPI.

The existing simplified methods, such as Seed et al. (1985), Robertson and Wride (1998) and Youd et al. (2001), were originally developed for clean sands. For the evaluation of sands with significant fines content (FC), the concept of ''equivalent clean sand'' was employed, suggesting that liquefaction resistance would increase as the FC increases. This concept is reflected in the three boundary curves corresponding to three ranges of fines content ($FC \leq 5\%$, $5\% < FC \leq 35\%$, and $FC > 35\%$) recommended by Seed et al. (1985), which has been well accepted by the profession. However, liquefaction of soils with high fines content (as high as 90%) in the past earthquakes has been observed (Kishida, 1969; Tohno and Yasuda, 1981; Bray et al., 2004). Laboratory cyclic simple shear tests, cyclic ring-shear tests, and cyclic triaxial tests of these soils (for example, Ishihara, 1993; Perlea et al., 1999; Guo and Prakash, 1999; Gratchev et al., 2006) suggest that the soil plasticity, and not necessarily the fines content alone, plays a major role in the liquefaction resistance behavior, i.e., the liquefaction resistance increases as the plasticity index increases. On the other hand, for sands with significant non-plastic fines content, the effect of fines content on the liquefaction resistance is less conclusive based on laboratory cyclic test results (for example, Carraro et al., 2003; Thevanayagam et al., 2000).

Since the Robertson and Wride (1998) method is widely used, one concern has been raised regarding the validity of using their simplified form of soil behavior type index I_c (where porewater pressures are omitted) as a proxy to the effect of fines on liquefaction resistance (Idriss and Boulanger, 2004, 2006). To ease this concern, Moss et al. (2006) suggested use of friction ratio ($R_f = f_s/q_t$) in lieu of I_c to account for the effect of fines, whereas Li et al. (2007) and Shuttle and Cunning (2007) suggested using a version of I_c that includes excess pore pressure ratio in the formulation. The excess porewater pressure ratio B_q, defined in NOTATION along with other CPTu parameters, correlates well with the behavior of fine-grained soils and has been incorporated into soil classification charts (Robertson, 1990; Jefferies and Davies, 1993). Thus, inclusion of B_q in the formulation of I_c appears suitable for extending the existing CPT-based evaluation from sands and silty sands to soils that are described as ''too clay-rich to liquefy.'' A CPT-based method that can evaluate the liquefaction resistance of soils over a *wide range* of I_c values would enable a more meaningful modeling of liquefaction effects within the framework of LPI.

In this study, the effects of CPT measured porewater pressures on soil liquefaction resistance are investigated through a study of case histories by considering the soil behavior type index I_c as defined by Jefferies and Davies (1993). In essence, knowledge is ''extracted'' from collected case histories using an artificial neural network (ANN), a well-established technique that can learn from examples (Rumelhart et al., 1986). This knowledge is then used to develop a new simplified model based on piezocone penetration testing (CPTu). The developed CPTu-based model is assessed and demonstrated with recent liquefaction case histories. Finally, it should be emphasized that the proposed CPTu model is not entirely new; it is built on the foundation of the previous work by many investigators.

LEARNING FROM CASE HISTORIES-ARTIFICIAL NEURAL NETWORK

Artificial Neural Network Approach for Liquefaction Evaluation

Training an artificial neural network (ANN) to approximate a highly nonlinear relationship for predicting the occurrence of liquefaction/no-liquefaction has been reported by various researchers (Goh, 1994; Agrawal et al., 1995; Goh, 1996; Juang et al., 1999a). In these previous studies, ANNs were trained using databases of case histories in which field observation, in the binary form of ''yes'' or ''no,'' was available. If the ANN has ''learned'' adequately from case histories, it may then be used for ''forecasting'' whether liquefaction could occur under a given scenario. Thus, the trained ANN may be used as a tool for assessing liquefaction potential of a soil in a given seismic loading. Recently, Juang et al. (2000, 2003) took this approach a step further. They developed a procedure with which the *limit state* for liquefaction triggering, commonly expressed as a boundary curve, can be established based on the trained ANN. It should be noted that the limit state for liquefaction triggering is essentially a model of CRR at a given CSR. Other ANN-based models developed for CRR have also been suggested (e.g., Kim and Kim, 2006).

Selection of Input and Output Variables

To learn effectively from a data set of case histories, choices must be made regarding the types of information to include from each case. Previous studies (e.g., Goh, 1994; Juang et al., 1999a) provide adequate guidance here. Each case history is an ''instance'' (data point) where the input consists of soil and earthquake data and the output consists of a field observation. The field observation is generally represented by only one variable, li-

quefaction indication (LI), in which LI = 1 for cases with surface manifestations of liquefaction (e.g., sand boiling, ground settlement, and lateral spreading) and LI = 0 for cases without surface manifestations of liquefaction. The following paragraphs detail the selection process for the input variables.

Selecting CSR as an input variable is the obvious choice because, in any cyclic stress-based method that follows the simplified procedure of Seed and Idriss (1971), CSR is used to characterize the earthquake load for assessing liquefaction potential. Throughout this paper, the variable CSR is the adjusted cyclic stress ratio as defined by Idriss and Boulanger (2004, 2006). It is expressed as:

$$\mathrm{CSR} = 0.65\left(\frac{\sigma_v}{\sigma'_v}\right)\left(\frac{a_{max}}{g}\right)(r_d)\left(\frac{1}{\mathrm{MSF}}\right)\left(\frac{1}{K_\sigma}\right) \quad (1)$$

where σ_v and σ'_v are the total stress and the effective stress, respectively, of the soil of concern at a given depth, g is the acceleration of gravity, which is the unit for peak ground surface acceleration a_{max}, r_d is the depth-dependent shear stress reduction factor, MSF is the magnitude scaling factor, and K_σ is the overburden correction factor for cyclic stress ratio. Both σ_v and σ'_v are in same units, and r_d, MSF, and K_σ are dimensionless. It should be noted that this definition of CSR (Eq. (1)) is already adjusted to the conditions of moment magnitude $M_w = 7.5$ and $\sigma'_v = 100$ kPa. This adjustment is essential to process case histories that were collected from different earthquakes of various magnitudes and to unify the influence of confining pressures. The intermediate parameters, r_d, K_σ, and MSF as defined by Idriss and Boulanger (2006) are employed herein.

It should be noted that various forms of CSR are available in the literature and differ primarily in the formulation of their intermediate variables, r_d, K_σ, and MSF. Please reference Youd et al. (2001) and Idriss and Boulanger (2006) for detailed discussions of these intermediate variables. However, a previous study by Juang et al. (2006), and a sensitivity analysis performed in this study showed that CSR values, determined with the formulation by Idriss and Boulanger (2006), agreed well with those obtained using the formulation recommended by Youd et al. (2001).

In addition to the data of earthquake loading as represented by CSR, the data of liquefaction resistance are needed to completely characterize a case history. Selecting the most suitable input variables to characterize liquefaction resistance of soils based on CPTu measurements is not a trivial task. In a CPTu, profiles of cone tip resistance q_t, sleeve friction f_s, and porewater pressure u_2 are recorded. Various derived dimensionless parameters are used to characterize the soils encountered in the CPTu measurement, including friction ratio R_f, normalized cone tip resistance Q_t, excess pore pressure ratio B_q, and normalized friction ratio F (Robertson, 1990; Jefferies and Davies, 1993). Additional derived parameters such as stress-adjusted cone tip resistance q_{t1N} and soil behavior index I_c (note: as is discussed later, different formulations of I_c are found in the literature; for example, Jefferies and Davies, 1993; Robertson and Wride, 1998) have also been used. These CPTu parameters are defined in NOTATION.

Using knowledge from previous studies (Juang et al., 2000, 2003, 2006), and the results of practically exhaustive analyses using ANNs with tens of different combinations of parameters in this study, two derived parameters, q_{t1N} and I_c, are judged most suitable for use as input variables for the intended ANN model.

The adjusted cone tip resistance q_{t1N} is determined as follows (Idriss and Boulanger, 2004, 2006):

$$q_{t1N} = C_N\, q_t/\sigma_{atm} \quad (2a)$$

$$C_N = \left[\frac{\sigma_{atm}}{\sigma'_v}\right]^{\alpha} \le 1.7 \quad (2b)$$

$$\alpha = 1.338 - 0.249(q_{t1N})^{0.264} \quad (2c)$$

where σ_{atm} is the atmosphere pressure (1 atm = 1.013 bars = 101.3 kPa).

Use of Eq. (2) requires a simple iterative procedure, as C_N and q_{t1N} are inter-dependent on the exponent α. Equation (2) was proposed by Idriss and Boulanger (2004, 2006) in conjunction with their CPT-based method for evaluation of liquefaction resistance of *sands*. This equation was derived using the concept of ''state'' parameter and an empirical relationship with relative density (Boulanger and Idriss, 2004). However, in this paper, the parameter q_{t1N} is used to capture the resistance behavior of clean sands and the effect of fines type and content is included by the soil behavior type index I_c. The choice of q_{t1N} as defined in Eq. (2), in contrast to other normalization models such as Olsen (1997) and Robertson and Wride (1998), is based on the fact that it produced the best results in the ANN learning of case histories.

The parameter I_c used in this paper is defined as follows (after Jefferies and Davies, 1993; Jefferies and Been, 2006, with a very slight modification as noted below):

$$I_c = \sqrt{[3 - \log_{10}\{Q_t(1 - B_q) + 1\}]^2 + [1.5 + 1.3(\log_{10} F)]^2} \quad (3)$$

It should be noted that in the original 1993 formulation, the bracket $\{Q_t(1 - B_q) + 1\}$ was expressed as $\{Q_t(1 - B_q)\}$. The value ''1'' is added here to prevent the bracket from becoming negative should B_q be greater than 1 (in such cases, Q_t is very small and $\{Q_t(1 - B_q)\}$ is less than 1). Moreover, according to Shuttle and Cunning (2007), the dimensionless term $\{Q_t(1 - B_q) + 1\}$ is ''fundamental for the evaluation of undrained response during CPTu sounding,'' which allows for greater differentiation between silty clays and clayey silts.

It should also be noted that the more well-known soil behavior type index used in the Robertson and Wride (1998) method is actually a simplification of the original 1993 form for sandy soils. The inclusion of B_q in the formulation of I_c in this paper is essential to allow the evaluation of liquefaction resistance to accommodate a wider range of soils. To avoid confusion, the soil behavior index determined with the Robertson and Wride's formulation is denoted in this study as $I_{c,\,RW}$. The formulation of this index $I_{c,\,RW}$ is listed in NOTATION.

In summary, three input variables (CSR, q_{t1N}, and I_c as per Eqs. (1), (2), and (3), respectively) and one output variable (LI) are employed to characterize a case history. After processing all case histories into a data set of instances, a three-layer, feed-forward artificial neural network is trained to approximate the following function: LI $= f(q_{t1N}, I_c, \text{CSR})$.

Database for Development of Artificial Neural Network

A database of case histories, consisting of 190 liquefied cases and 123 non-liquefied cases, was compiled from five well-documented sources (Moss et al., 2006; Ku et al., 2004; Lai et al., 2004; Bray et al., 2004; PEER, 2007). These cases were derived from the 1964 Niigata, Japan earthquake ($M_w = 7.5$), the 1976 Tangshan, China earthquake ($M_w = 8.0$), the 1977 Vrancea, Romania earthquake ($M_w = 7.2$), the 1979 Imperial Valley, California earthquake ($M_w = 6.5$), the 1980 Mexicali, Mexico earthquake ($M_w = 6.2$), the 1983 Borah Peak, Idaho earthquake ($M_w = 6.9$), the 1987 Edgecumbe, New Zealand earthquake ($M_w = 6.6$), the 1987 Elmore Ranch, California earthquake ($M_w = 6.2$), the 1987 Superstition Hills, California earthquake ($M_w = 6.6$), the 1989 Loma Prieta, California earthquake ($M_w = 7.0$), the 1995 Hyogoken-Nanbu, Japan earthquake ($M_w = 7.2$), the 1999 Chi-Chi, Taiwan earthquake ($M_w = 7.6$), and the 1999 Kocaeli, Turkey earthquake ($M_w = 7.4$). The binary criterion of liquefaction/no-liquefaction was primarily based on surface manifestation of liquefaction, such as sand boils, ground settlement, and lateral spreading (or lack thereof), and in some cases (such as those reported by Bray et al., 2004), critical layers were identified by field observations supplemented with detailed dynamic finite element analyses or confirmed by multiple existing liquefaction evaluation methods.

Figure 1 shows the soils in these cases in the soil behavior type classification chart. Table 1 shows the soil behavior types and their ranges of I_c values defined by Jefferies and Davies (1993) and employed in this study. Table 2 shows the ranges of the values of various parameters in these cases. Together, Fig. 1 and Tables 1 and 2 characterize the database used in this paper. This database is available from the first writer upon request.

It should be noted that the CPT data reported in the database of Moss et al. (2006) did not include B_q. An examination of all other CPTu data revealed that for those cases with $I_{c,RW} < 2.2$ and friction ratio $R_f < 1.5\%$, the values of B_q are very small ($-0.06 < B_q < 0.02$). Assuming $B_q = 0$ for these cases will cause a maximum error in the computed I_c of less than 2%. Thus, the database from Moss et al. (2006) was screened with the criteria of $I_{c,RW} < 2.2$ and $R_f < 1.5\%$, and 116 cases were selected. These cases are assumed to have $B_q = 0$ and are included in the new database for the present study. The rest of the data in this new database were derived from the 1999 Chi-Chi, Taiwan Earthquake and the 1999 Kocaeli, Turkey Earthquake where B_q was directly included.

Training and Testing of Artificial Neural Network

In ANN terminology, a three-layer, feed-forward neural network consists of an *input* layer, an *output* layer and a *hidden* layer. For each case in the database, the input layer consists of three *neurons* (representing q_{t1N}, I_c, and CSR, respectively) and the output layer consists of one neuron (representing LI). The goal of ANN learning from case histories is to map the input layer to the output layer by determining the connection weights and biases

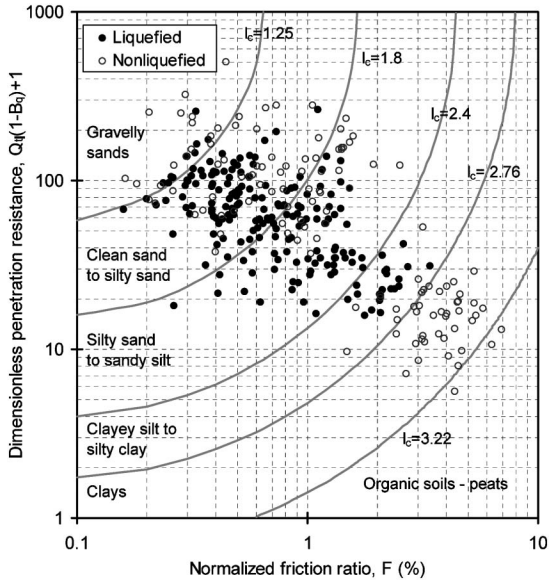

Fig. 1. Case histories in the database plotted on the CPT soil behavioral classification chart (after Juang et al., 2008)

Table 1. Soil behavior types by the index I_c (after Jefferies and Davies, 1993)

Range of I_c (Equation 3)	Zone (or type)	Soil classification
$I_c < 1.25$	7	Gravelly sands
$1.25 \le I_c < 1.80$	6	Sands: clean sand to silty sand
$1.80 \le I_c < 2.40$	5	Sand mixture: silty sand to sandy silt
$2.40 \le I_c < 2.76$	4	Silt mixture: clayey silt to silty clay
$2.76 \le I_c < 3.22$	3	Clays
$I_c \ge 3.22$	2	Organic soils and peats

Table 2. Ranges of values of various parameters in case histories

	Depth (m)	q_t (MPa)	f_s (kPa)	u_2 (kPa)	R_f (%)	F (%)	σ_v (kPa)	σ'_v (kPa)	q_{t1N}	B_q	I_c	a_{max} (g)	M_w	CSR
Max	20.0	23.9	456	421	5.9	6.9	370	263	217	0.3	3.2	0.70	8.0	0.83
Min	1.3	0.4	3	−104	0.1	0.1	22	17	7	−0.2	0.9	0.09	5.9	0.05

through an error reduction process (Juang et al., 1999a). This is expressed as:

$$\mathrm{LI} = f_{\mathrm{T}}\left\{B_0 + \sum_{\mathrm{k}=1}^{n}\left[W_{\mathrm{k}} \cdot f_{\mathrm{T}}\left(B_{\mathrm{Hk}} + \sum_{\mathrm{i}=1}^{m} W_{\mathrm{ik}} P_{\mathrm{i}}\right)\right]\right\} \quad (4)$$

where B_0 is bias at the output layer (only one neuron in this layer), W_{k} is weight of the connection between neuron k of the hidden layer and the single output layer neuron, B_{Hk} is bias at neuron k of the hidden layer ($k = 1, n$), W_{ik} is weight of the connection between input variable i ($i = 1, m$) and neuron k of the hidden layer, P_{i} is input parameter i, and $f_{\mathrm{T}}(\theta)$ is a transfer function defined as: $f_{\mathrm{T}}(\theta) = 1/(1 + e^{-\theta})$ where θ is a dummy variable.

The number of input variables, m, is equal to 3 in this ANN. Thus, $P_1 = q_{\mathrm{t1N}}$, $P_2 = I_{\mathrm{c}}$, and $P_3 = \mathrm{CSR}$. The number of hidden neurons is determined through a trial-and-error process; in the present study, the number of neurons is chosen to be 7 based on numerous experiments with the goal of securing high success rate (defined later) and repeatability in training and testing.

As in the conventional approach, two-thirds of the instances (cases) in the database are used as the training data set and the rest are used as the testing data set. In principle, ANN is trained with *only* the training data set, and the trained ANN is then examined for how well it generalizes the input-output relationship using a testing data set that was *not* employed in the training. Numerous trials have also been performed with different combinations of training and testing data to ensure *repeatability* of the trained ANN. The repeatability is important as the desired network must be stable and yield consistent results. In the present study, the Levenberg-Marquardt (LM) algorithm is adopted for its efficiency in training networks. The LM algorithm, illustrated in Fig. 2, yields an update of weights and biases (denoted here as $x_{\mathrm{k}+1}$) as follows:

$$x_{\mathrm{k}+1} = x_{\mathrm{k}} - [J^{\mathrm{T}}J + \mu I]^{-1} J^{\mathrm{T}} e \quad (5)$$

where x_{k} and $x_{\mathrm{k}+1}$ are the previous and the updated vectors of weights and biases, respectively; J is the Jacobian matrix that contains the first derivatives of the network errors with respect to the weights and biases; μ is a scalar that is decreased after each successful step (in reduction of the performance function), I is the identity matrix, and e is a vector of network errors. Further details about the implementation of the LM algorithm can be found in Hagan and Menhaj (1994) and the neural network toolbox of MATLAB (MathWork, Inc., 2002; Demuth and Beale, 2002).

Because the output of the ANN is an indication of liquefaction, the success rate of the trained network in ''predicting'' whether or not liquefaction occurred in each of the cases in the database can be used to characterize the performance of the developed ANN. In the present study, multiple ANNs are found to yield satisfactory success rates ($\approx 90\%$). Although any of these ANNs may be used for ''predicting'' whether liquefaction will occur for a given soil under a given seismic loading, additional criterion is put in place in this study to select the most desirable ANN. This criterion is based on how well boundary surface or limit state surface generated by the developed ANN can delineate liquefied cases from non-liquefied cases. This point will be discussed later in detail.

BOUNDARY SURFACE SEARCHED WITH AID OF NEURAL NETWORK

The search procedure that utilizes ANN for locating data points on the unknown *boundary surface*, referred to herein as the limit state surface, was developed by Juang et al. (2000). The concept behind this procedure is very simple. For each case in the database, if liquefaction is observed (output LI = 1), the search for a point on the boundary surface involves a gradual reduction of CSR or a gradual increase in q_{t1N}. Each search, if successful, results in a three-dimensional data point (CSR, q_{t1N}, I_{c}) that is located on the unknown boundary surface. The

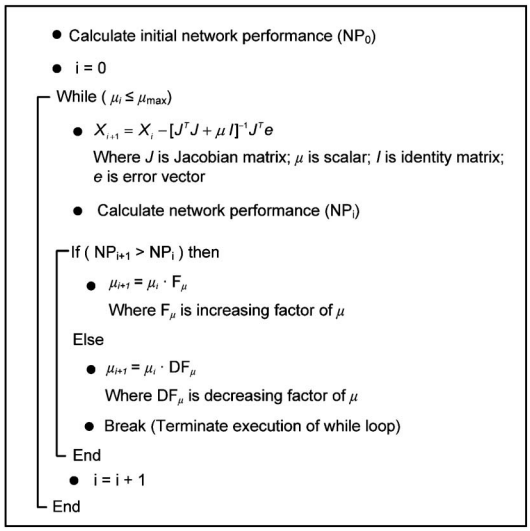

Fig. 2. Levenberg-Marquardt algorithm for neural network training

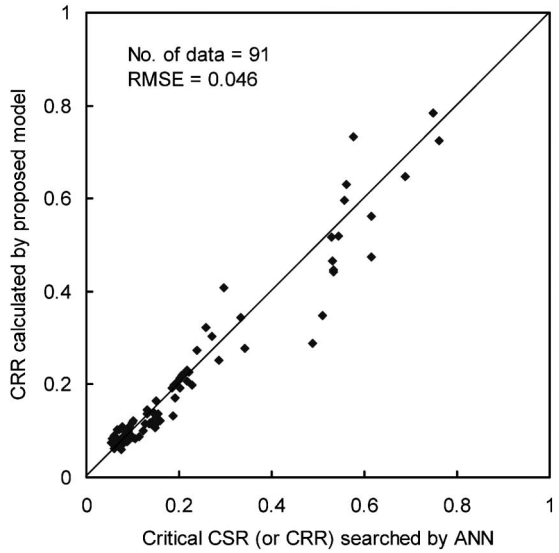

Fig. 3. Scatter of the CRR predictions using the proposed model

CSR of this ''searched'' data point is referred to herein as the *critical* CSR, and by definition, the critical CSR on the limit state surface is the CRR for the given soil conditions represented by q_{t1N} and I_c. Thus, a limit state function CRR = $f(q_{t1N}, I_c)$ can be established once a large number of data points have been ''found'' through the search. In this study, 91 data points were successfully generated.

As noted previously, the success rate of the developed ANN in ''predicting'' the occurrence/no-occurrence of liquefaction in the case histories examined is one indication of the performance of this ANN. However, the success rate examines *only* the performance of the developed ANN with data employed. To see how well the trained ANN has *generalized* the input-output relationship, an additional check is desirable. The data points on the unknown boundary surface generated from the trained ANN may be used to assess the adequacy of neural network generalization. This can be carried out in two steps. Least-square regression is first performed on the generated data to establish an empirical model, CRR = $f(q_{t1N}, I_c)$, of the boundary surface. The boundary surface is then examined to see how well liquefied and non-liquefied cases can be delineated by this surface. A satisfactory ANN must have a satisfactory success rate and the generated boundary surface must be able to delineate liquefied cases from non-liquefied cases.

A series of least-squares regression analyses were con-

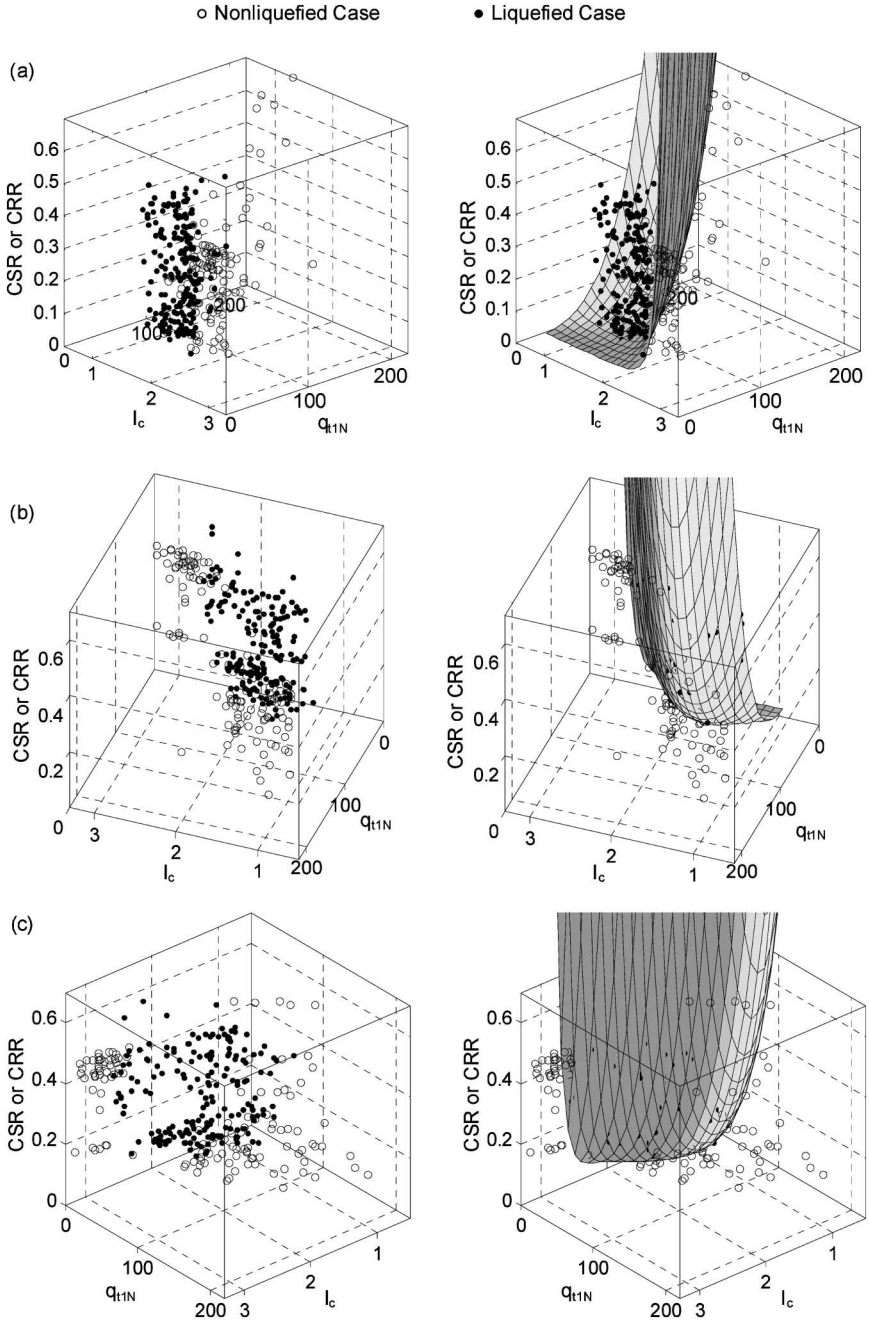

Fig. 4. Boundary surface at three different angles with case history data (after Juang et al., 2008)

ducted on the 91 boundary-surface data points that were ''found'' in the search process using the developed ANN model. The following least-squares expression was obtained (in reference to Fig. 3):

$$\mathrm{CRR} = 0.05 + \exp\left[A + B \times (q_{t1N}/100)^{C}\right] \quad (6)$$

where

$$A = I_c \cdot (q_{t1N}/100) - 10.455$$
$$B = 0.669 \cdot I_c^3 - 5.55 \cdot I_c + 12.993$$
$$C = 0.284 - 0.0214 \cdot I_c^2$$

and where q_{t1N} is per Eq. (2) and I_c is per Eq. (3). These

Table 3. Success rates of the ANN-generated CRR model by category

Range of I_c	No. of cases	Success rate
$I_c < 1.25$	25	96%
$1.25 \le I_c < 1.80$	126	86%
$1.80 \le I_c < 2.40$	96	96%
$I_c > 2.40$	66	86%
All cases	313	90%
Liquefied group	190	100%
Non-liquefied group	123	74%

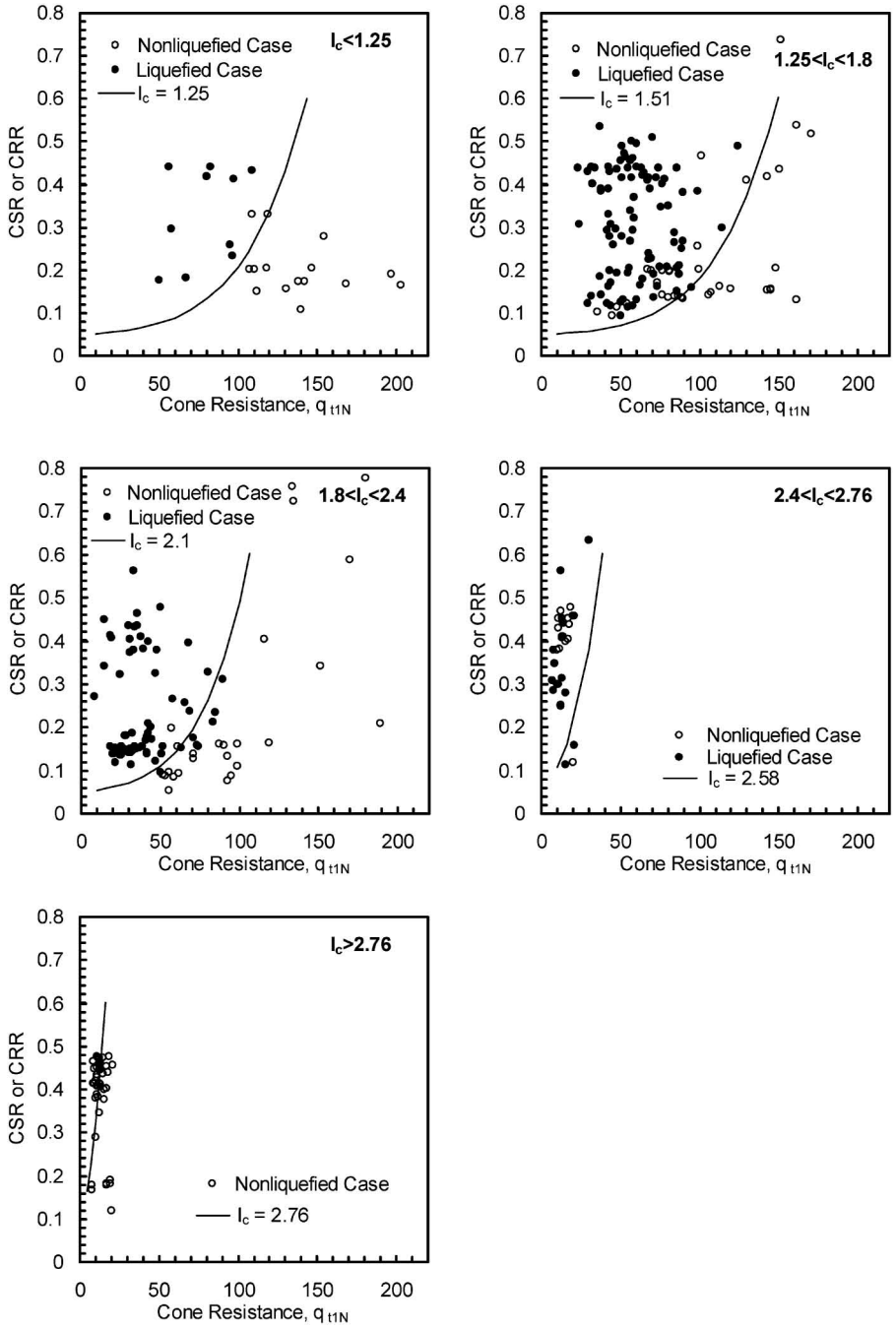

Fig. 5. 2-D graphs of the proposed model–CRR (or CSR) versus q_{t1N} (Eq. (2))

definitions must be strictly followed whenever Eq. (6) is employed for evaluating CRR, and the resulting CRR must be compared to CSR defined in Eq. (1) for assessing liquefaction potential, as Eqs. (1), (2), (3) and (6) were calibrated as a whole in the ANN learning and interpolation.

In short, the proposed CPTu-based method involves evaluation of CSR by Eq. (1) and CRR by Eqs. (2), (3), and (6). The liquefaction potential is then assessed with factor of safety (F_S) defined as $F_S = \text{CRR}/\text{CSR}$.

The developed boundary surface (CRR model expressed in Eq. (6)) is then examined to see whether it can delineate liquefied cases from non-liquefied cases. Figure 4 shows three dimensional (3-D) graphs of case history data points in different angles in space, with and without the boundary surface. While not shown herein, the 3-D graph can be rotated in a Matlab window from 0° to 360° and thus unlimited number of ''views'' of the boundary surface can be shown to observe the performance of this ANN-generated boundary surface. Based on these views, the same conclusion can be reached: the ANN-generated boundary surface can delineate liquefied cases from non-liquefied cases in the 3-D space.

The capability of the developed CPTu-based model to delineate liquefied cases from non-liquefied cases has been demonstrated with the 3-D graphs shown in Fig. 4. The accuracy of this model is also revealed in the success rates in ''predicting'' both liquefied and non-liquefied cases, listed in Table 3. Much higher success rates in predicting liquefied cases than non-liquefied cases, shown in this table, implies that the developed model is conservatively biased, which is desirable for engineering applications using a deterministic approach. The degree of this conservative bias will be examined later.

CAPABILITY AND ACCURACY OF PROPOSED CPTu-BASED METHOD

It is desirable to compare the new CPTu-based method with the existing methods. Because the existing boundary curves (CRR models) are all presented in 2-D graphs, it is necessary to present the developed model accordingly. Figure 5 depicts the CRR model at selected I_c levels, where the boundary surface becomes a boundary curve. Also shown in this figure are case history data points within the corresponding ranges of I_c. Because each boundary curve is derived from Eq. (6) by setting I_c at the midpoint of the corresponding range of I_c, the examination of the ''performance'' of boundary curves with these data points is seen *only* as an approximation. Nevertheless, the results presented in Fig. 5 clearly show the capability and accuracy of the developed CRR model. It is noted that as I_c increases beyond 2.4, in which q_{t1N} is generally small, the ability of the CRR-q_{t1N} boundary curve to delineate liquefied cases from non-liquefied cases reduces drastically. Thus, for soils with high I_c, which generally have low q_{t1N} values ($q_{t1N} < 40$), the traditional 2-D graphs of CRR (or CSR) versus q_{t1N} offer little information. On the other hand, for these soils, a plot of CRR

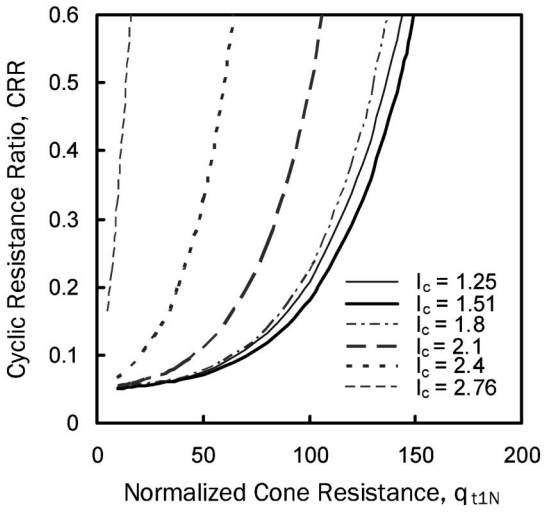

Fig. 6. Family boundary curves of the proposed model–CRR versus q_{t1N} (Eq. (2))

(or CSR) versus I_c, presented later, can help delineate liquefied cases from non-liquefied cases. This suggests that for soils with high I_c and low q_{t1N}, the variable I_c has a much greater influence on liquefaction resistance than the variable q_{t1N}.

Figure 6 shows a set of ''family'' CRR-q_{t1N} boundary curves that correspond to different soil types implied by I_c. Each of the boundary curves represents the intersection of a given plane I_c = constant (say, $I_c = 1.51$) and the boundary surface (Eq. (6)) in the 3-D space. One interesting observation is that *for a given* q_{t1N}, the liquefaction resistance is the lowest at $I_c \approx 1.51$, which is approximate at the *midpoint* of the range of I_c for ''sands'' (where the lower end of the range is $I_c = 1.25$ for gravelly sand, and the higher end is $I_c = 1.8$ for silty sand; *see* Table 2). The soils with lower I_c, such as ''gravelly sands'' ($I_c \leq 1.25$), is found to have higher liquefaction resistance than those soils with $I_c \approx 1.51$ (clean sands). In other words, for soils with the same q_{t1N}, the liquefaction resistance increases as I_c decreases from 1.51 to 1.25. It is easily understood as the soils in this range ($I_c = 1.25$ to 1.51) contain practically no fines, and the liquefaction resistance increases with the increase in the particle size and strength. On the other hand, for soils with the same q_{t1N}, the liquefaction resistance increases as I_c increases from 1.51 to 1.8 (Fig. 6), which is also easily understood as the soils in this range [from $I_c = 1.51$ (clean sand) to 1.8 (silty sand)] tend to have greater liquefaction resistance due to the effect of the fines. Thus, the CPTu model developed in this paper is different from the Robertson and Wride (1998) method; the latter artificially set a lower bound at $I_{c,\,RW} = 1.64$ (clean sand) for liquefaction resistance evaluation. In other words, the Robertson and Wride (1998) method implicitly assumed that soils with $I_{c,\,RW} < 1.64$ would have the same liquefaction resistance as those with $I_{c,\,RW} = 1.64$.

Similar to the 2-D graphs of CRR versus q_{t1N} presented previously, a separate set of 2-D graphs depicting the re-

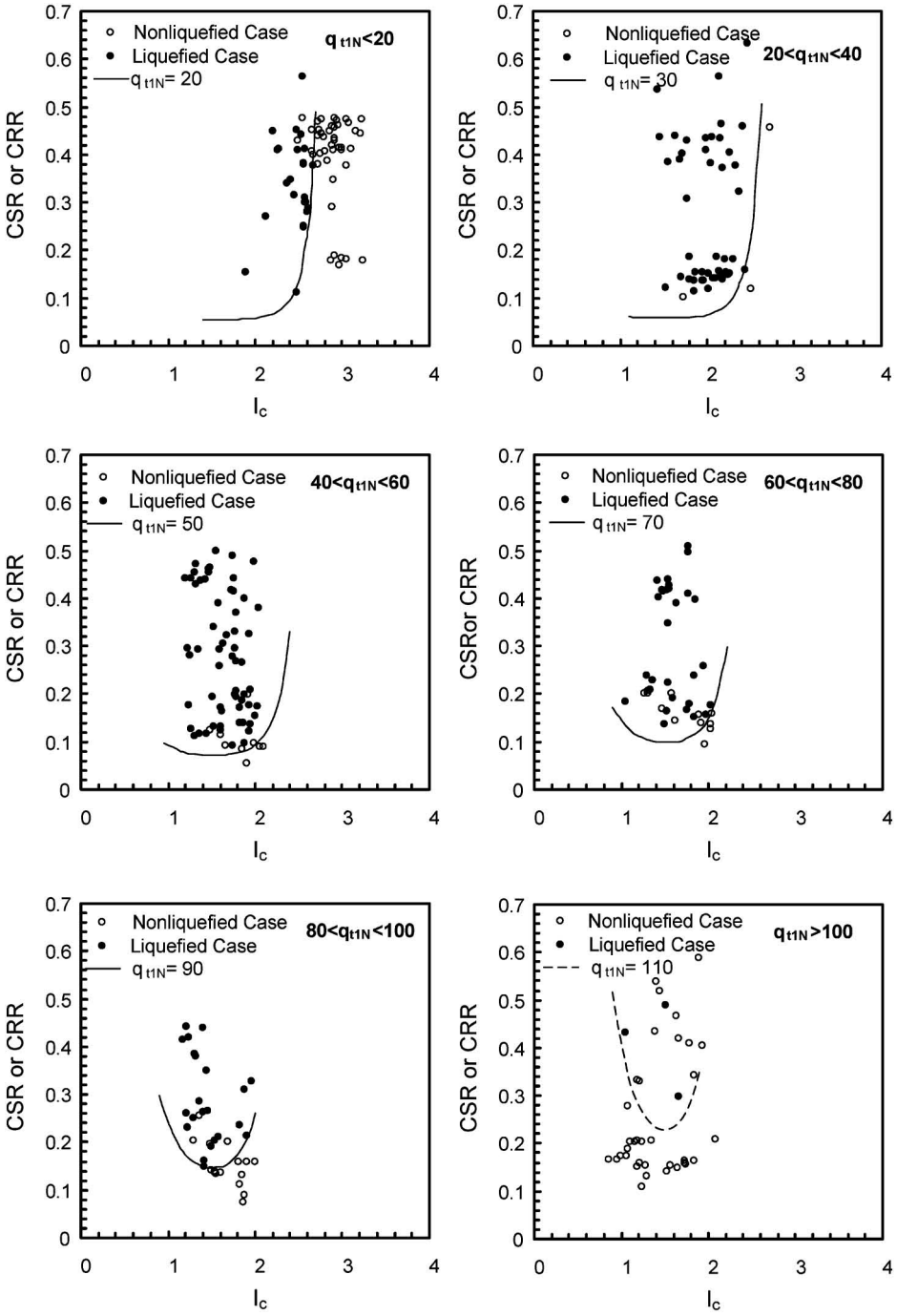

Fig. 7. 2-D graphs of the proposed model–CRR (or CSR) versus I_c (Eq. (3))

lations between CRR and I_c at various q_{t1N} levels can also be derived from Eq. (6). Figure 7 shows these 2-D graphs with case histories, which demonstrate again that the developed CRR model can delineate liquefied cases from non-liquefied cases. It should be noted that the boundary curves shown in Fig. 7 represent an interpretation of ''behavior'' of the data by the trained ANN model. These boundary curves were not visually drawn based on the 2-D data points. The data points were super-imposed onto each chart merely for verifying whether the boundary curve can delineate liquefied cases from non-liquefied cases. It is noted that for the chart with $q_{t1N} > 100$, at the lower right part of Fig. 7, the boundary curve is presented in dashed curve, indicating that it has not been verified with sufficient data points.

Furthermore, the ability to delineate liquefied cases from non-liquefied cases at lower q_{t1N} levels (say, less than 40) with these CRR-I_c boundary curves is particularly important as it complements the inability of the CRR-q_{t1N} boundary curve to delineate liquefied cases from non-liquefied cases at these lower q_{t1N} levels. Again, this indicates that for soils with high I_c and low q_{t1N}, the variable I_c has a much greater influence on liquefaction resistance than the variable q_{t1N}. On the other hand, these graphs

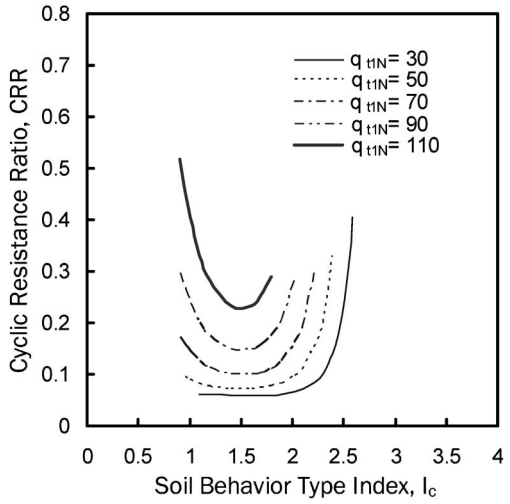

Fig. 8. Family boundary curves of the proposed model–CRR versus I_c (Eq. (3))

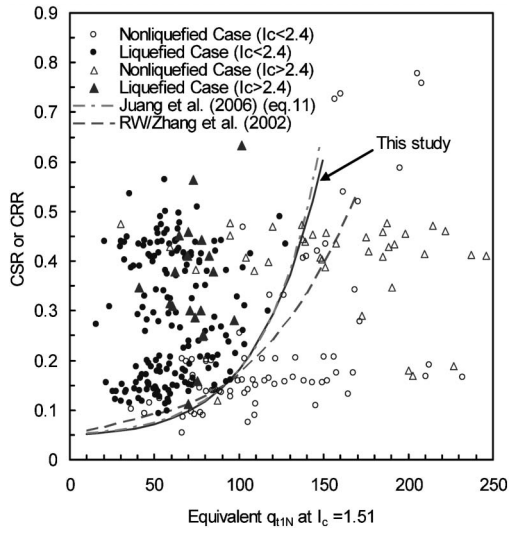

Fig. 9. Base boundary curve with transformed data

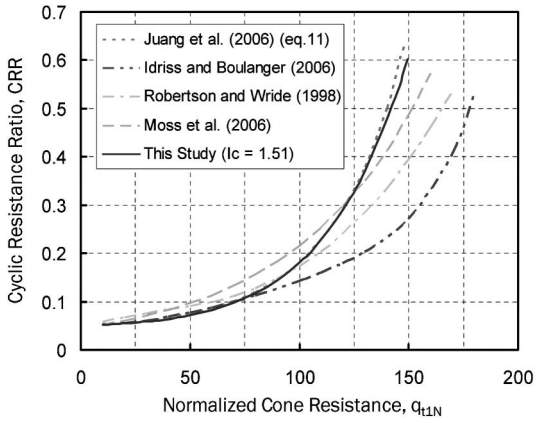

Fig. 10. Comparison of base boundary curves from various models

also show that for soils with higher q_{t1N} (and generally lower I_c), variable q_{t1N} has a much greater influence on liquefaction resistance than variable I_c.

Figure 8 presents a set of ''family'' CRR-I_c boundary curves that correspond to various q_{t1N} levels. This figure clearly shows that for a given q_{t1N}, the liquefaction resistance is the lowest at $I_c \approx 1.51$.

Finally, it is of interest to show all case histories with different soils in the same 2-D graph of CRR (or CSR) versus q_{t1N}, at least from a historic perspective. This necessitates the development of the so-called ''clean sand equivalence'' of cone tip resistance for any given soil. Robertson and Wride (1988) developed a correction factor K_c that can be applied to the normalized cone tip resistance q_{c1N} to yield the ''clean sand equivalence,'' $q_{c1N,\,cs}$. Their idea was to transform an empirical model, $CRR = f(q_{c1N}, I_{c,\,RW})$, into a new model, $CRR = f(q_{c1N,\,cs})$, subject to the constraint that both models yield the same liquefaction resistance. In the procedure recommended by Robertson and Wride (1988), the correction factor K_c is a function *only* of $I_{c,\,RW}$. However, as discussed previously, at different levels of q_{t1N}, the influence of I_c differs, and the correction factor K_c then becomes a function of both soil type (represented by I_c) and normalized cone tip resistance (q_{t1N}). Thus, development of an empirical model for K_c will be of little practical value, since such empirical equations would be as complicated as Eq. (6) and involving the same two input variables as required in Eq. (6). Nevertheless, numerical solutions for an equivalent q_{t1N} value at a reference level of $I_c = 1.51$ (where the liquefaction resistance is the lowest for a given q_{t1N}) can be obtained for all cases ($I_c \neq 1.51$) by satisfying the constraint: $f(q'_{t1N}, 1.51) = f(q_{t1N}, I_c)$ where q'_{t1N} is the equivalent q_{t1N} value at $I_c = 1.51$, and f is the function for CRR expressed in Eq. (6). Figure 9 shows all *transformed* data points along with the ''base'' boundary curve, which is obtained by plotting Eq. (6) at $I_c = 1.51$. The developed empirical model (Eq. (6)), presented as a boundary curve in this 2-D graph, is again shown to be able to delineate liquefied cases from non-liquefied cases.

For comparison, two other $I_{c,\,RW}$-based CRR models are shown in Fig. 9. It is important to emphasize that this comparison of the three boundary curves is *only approximate*, as the definition of the ''base'' boundary curves by Robertson and Wride (1998) and Juang et al. (2006) is not exactly the same as that adopted in this study. In addition, the CRR model developed in this study is based on CPTu, whereas the other two models are based on CPT. Nevertheless, the results show that the base boundary curve of the new model, in which the effect of B_q is negligible, is very comparable to those of the existing models. In fact, the base boundary curve of the new CPTu-based model is almost identical to that of Juang et al. (2006). This result is significant because the two models were developed with different formulations and databases.

Figure 10 further compares the base boundary curve with two additional models proposed by Moss et al. (2006) and Idriss and Boulanger (2006). Note that for the probabilistic model of Moss et al. (2006), an equivalent deterministic boundary curve is obtained by adopting a

15% probability as suggested by the authors. The results show that these base boundary curves are quite comparable, even though the Idriss and Boulanger curve appears conservative. At lower q_{t1N} (<80), the proposed model is consistent with the Idriss and Boulanger curve. As q_{t1N} increases to the level of $q_{t1N} \approx 100$, the proposed model catches up with the Robertson and Wride curve; as q_{t1N} continues to increase to the level of $q_{t1N} \approx 125$, the proposed model catches up with the Moss et al. curve. Cautions must be exercised, however, in drawing conclusions based on Fig. 10. *Firstly*, the above comparison is based on the 2-D view of the models (for the proposed model, it is the intersection of the boundary surface with the plane $I_c = 1.51$ in the 3-D space; and for other models, the base curves are assumed "equivalent" to the condition of $I_c = 1.51$). Because the proposed model is a boundary surface in the 3-D space, which is fundamentally different from the 2-D boundary curves, any such comparison in a 2-D graph should be viewed with caution, particularly in light of the results from Figs. 5 and 7. *Secondly*, although the base boundary curves are similar, these CPT-based models can yield contradictory conclusions on liquefaction resistance for silty or clayey soils because the effect of fines is treated differently.

EFFECT OF EXCESS PORE PRESSURE RATIO IN THE PROPOSED MODEL

The effect of CPTu-measured porewater pressures can be ascertained with the proposed CPTu method. Figure 11 shows the influence of ignoring the parameter B_q in the formulation of I_c on the calculated CRR. For a soil with a significant B_q, assuming $B_q = 0$ in Eq. (3) results in a different I_c value, denoted as $I_{c,\,B_q=0}$, which in turn results in a different CRR. The resulting difference (in percentage) in CRR is depicted in Fig. 11. If the true B_q is positive, ignoring B_q leads to an underestimation of CRR; conversely, if the true B_q is negative, ignoring B_q results in an overestimation. The percentage change in CRR (in reference to the CRR calculated from Eq. (6) with correct I_c) may be estimated with the following equation obtained by curve-fitting ($r^2 = 0.994$, RMSE = 1.8):

$$\%\ \text{change in CRR} = aB_q^4 + bB_q^3 + cB_q^2 + dB_q + 0.205 \quad (7)$$

where

$$a = 632.45\, I_{c,\,B_q=0}^2 - 3430.99\, I_{c,\,B_q=0} + 4554.91$$
$$b = -1640.85\, I_{c,\,B_q=0}^2 + 8558.12\, I_{c,\,B_q=0} - 10970.40$$
$$c = 1223.26\, I_{c,\,B_q=0}^2 - 5934.08\, I_{c,\,B_q=0} + 7139.90$$
$$d = -158.56\, I_{c,\,B_q=0}^2 + 445.25\, I_{c,\,B_q=0} - 248.53$$

For all data points shown in Fig. 11, the percentage change in CRR strongly correlates with the magnitude of B_q, as reflected in the extremely high r^2. Figure 12 shows the effect of B_q in different angles. As reflected in Eq. (7), the change in CRR is a function of B_q and $I_{c,\,B_q=0}$. As shown in Fig. 12, when $I_{c,\,B_q=0} < 2.0$ (approximately), the soil is probably in a drained condition during penetration, no significant excess pore pressure is observed and the percentage change in CRR as a result of ignoring B_q is generally small (i.e., $<2\%$). As $I_{c,\,B_q=0}$ increases beyond 2.0, there is a significant increase in B_q, indicating a possible change from the drained condition to the undrained condition. Thus, for soils with $I_{c,\,B_q=0} > 2.0$, ignoring B_q in

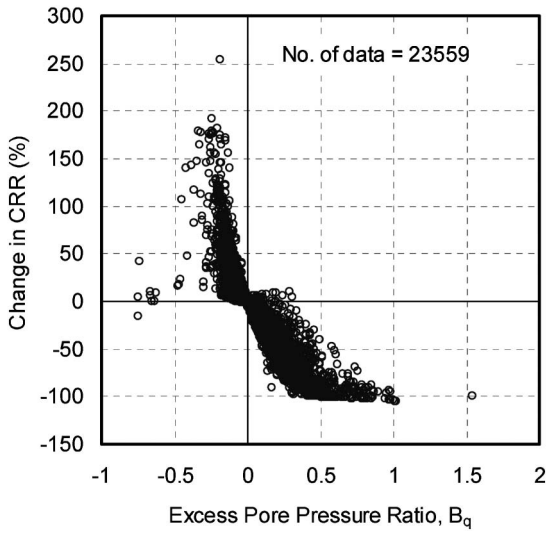

Fig. 11. Percentage change in CRR as a result of ignoring B_q in the proposed model

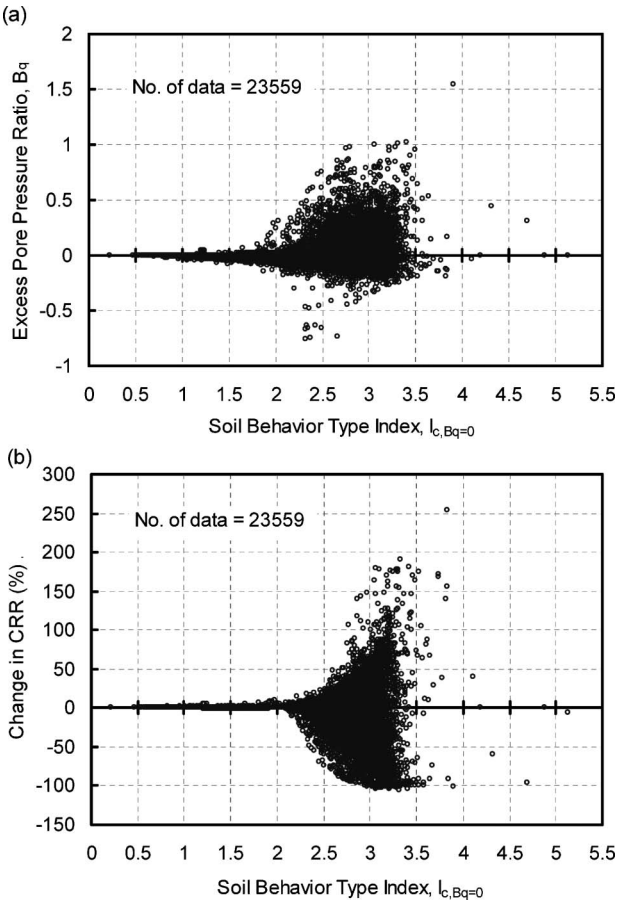

Fig. 12. Percentage change in CRR as a result of ignoring B_q –a different angle

the formulation of I_c (Eq. (3)) can lead to a significant error in the CRR calculated with Eq. (6). The aforementioned discussions address the effect of B_q (or the consequence of ignoring B_q) on CRR in the proposed CPTu-based model. It should be noted, however, that the effect of B_q on CRR in other existing CPT-based models may not be as pronounced. First, the existing CPT-based models are mainly developed for sandy soils, and for sands, $B_q \approx 0$. Second, the effect of B_q may have been compensated *to some degree* by a combined use of CPT parameters such as q_c, R_f, and $I_{c,RW}$. Nevertheless, this effect of B_q (through I_c) on CRR is very significant particularly for silt mixtures.

PROBABILITY AND FACTOR OF SAFETY CONSIDERATIONS

The proposed CPTu-based method is able to delineate liquefied cases from non-liquefied cases (Figs. 4, 5, 7, and 9 and Table 3). However, the success rate for liquefied cases (100%) is much greater than that for non-liquefied cases (74%), suggesting that the proposed model has a conservative bias. Thus, it is desirable to determine how conservative the proposed model is. A procedure to characterize a deterministic model in terms of probability based on a database of case histories has been developed by Juang et al. (1999b, 2002). This procedure involves an analysis of the distributions of F_S values for both liquefied and non-liquefied cases, respectively, followed by use of Bayes' theorem to create a mapping function that yields probability of liquefaction for a given F_S. Using this procedure, the following mapping function is developed in this study (RMSE ≈ 0.02):

$$P_L = \frac{1}{1 + e^{-3.64 + 5.37 F_S}} \tag{8}$$

It should be emphasized that the probability of liquefaction P_L determined with Eq. (8) is *conditioned* on a given F_S that is calculated with the proposed method (with CSR by Eq. (1) and CRR by Eq. (6)). The meaning of F_S determined with different models can greatly differ from each other since different degrees of conservatism may have been implemented in these models. For the proposed method, a factor of safety of $F_S = 1$ yields a conditional probability of liquefaction of 0.15 according to Eq. (8). This result confirms that the proposed method has a conservative bias. Previous studies (Cetin et al., 2004; Moss et al., 2006; Juang et al., 2006) have suggested an acceptable level of liquefaction probability of $P_L = 0.15$ for design of ordinary structures. Thus, when applying the proposed model in a deterministic analysis, a factor of safety of $F_S > 1.0$ is considered adequate for use in designing ordinary structures. In other words, no additional factor of safety is necessary when evaluating liquefaction potential at a site for ordinary structures using the proposed model. Should a more stringent level of tolerable risk ($P_L < 0.15$) be required, the minimum required F_S can be adjusted accordingly.

Finally, it should be noted that the conditional probability of liquefaction determined with Eq. (8) is a *nominal* probability, meaning that good standards of engineering practice are followed in both data acquisition and analysis, and possible uncertainties are adequately compensated in the derived data.

LIQUEFACTION POTENTIAL OF SILT MIXTURE–CASES STUDY

One unique feature of the proposed CPTu-based method is its capability to assess liquefaction potential of ''silt mixtures'' (i.e., clayey silt to silty clay) using the modified I_c that considers porewater pressure ratio (B_q). To this end, it is of interest to demonstrate this capability by back-analysis of well documented case histories from the August 17, 1999 Kocaeli earthquake that involved soils considered to be ''too clay-rich to liquefy.''

An extensive site investigation program, including 135 CPT profiles and 46 exploratory SPT borings with energy

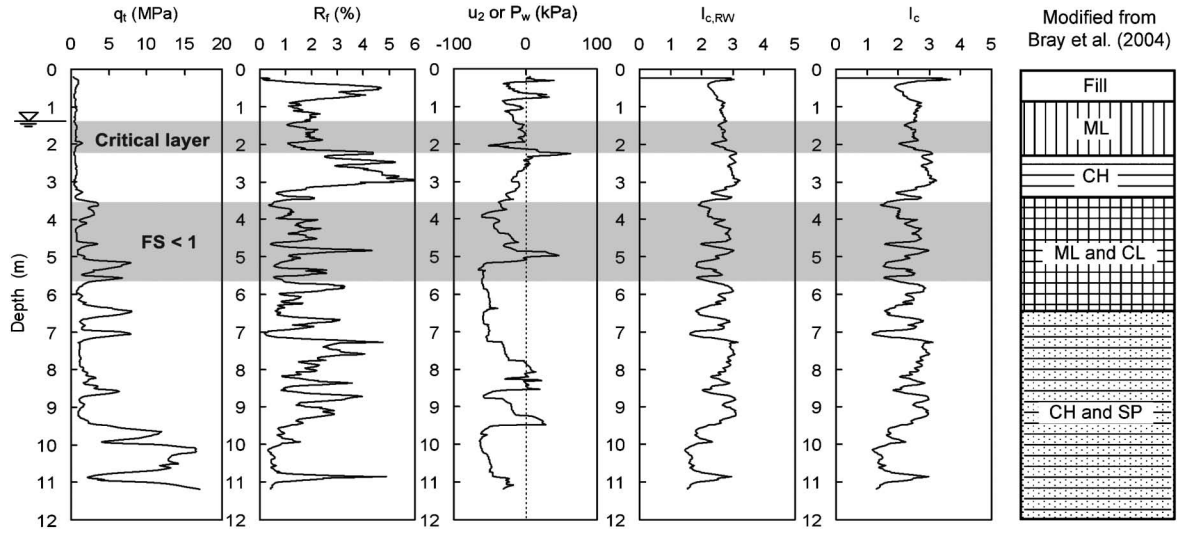

Fig. 13. CPTu sounding profiles and soil classification at location CPT-C4 in Adapazari (after Juang et al., 2008)

measurements, was conducted in Adapazari, Turkey after the Kocaeli earthquake (Bray et al., 2004). All available CPTu sounding profiles were analyzed in this study and similar results were obtained. Two sets of CPTu sounding profiles along with results of the analysis are presented as examples.

Figure 13 shows the profiles from CPTu sounding C4 which was conducted at the site of Building C2 (Bray et al., 2004). Included in this figure are q_t, R_f, u_2 (or P_w), $I_{c,RW}$, I_c, and soil classification as per an adjacent soil test boring. The critical layer marked in this figure is one that was judged to have liquefied in the 1999 earthquake by Bray et al. (2004) based on field observations and analysis of *in situ* test data. The layer marked with "$F_S < 1$" is the layer that was considered liquefiable by Bray et al. (2004) based on their analysis. It should be noted that the critical layer was later confirmed by detailed numerical analysis (Bray et al., 2006).

Using the CPTu data shown in Fig. 13 and the seismic parameters of $M_w = 7.4$ and $a_{max} = 0.40$ g, liquefaction potential in terms of factor of safety is calculated with both the proposed model and the RW/Zhang method, which is the shorthand of the Robertson and Wride (1998) method as updated in Zhang et al. (2002). Figure 14 shows the results of this analysis. In the critical layer where $I_{c,RW} > 2.6$, direct application of the RW/Zhang method (or the Robertson and Wride method), would yield "no liquefaction" (it should be noted that in case of $I_{c,RW} > 2.6$, Robertson and Wride actually suggested use of other criteria to confirm this assertion), whereas the application of the proposed method would yield F_S much less than 1, indicating "liquefaction." In this case, the results obtained by the proposed model agree with field observation. Overall, improved results are obtained using the proposed CPTu method directly without resort to further analyses.

Figures 15 and 16 show similar results obtained for the

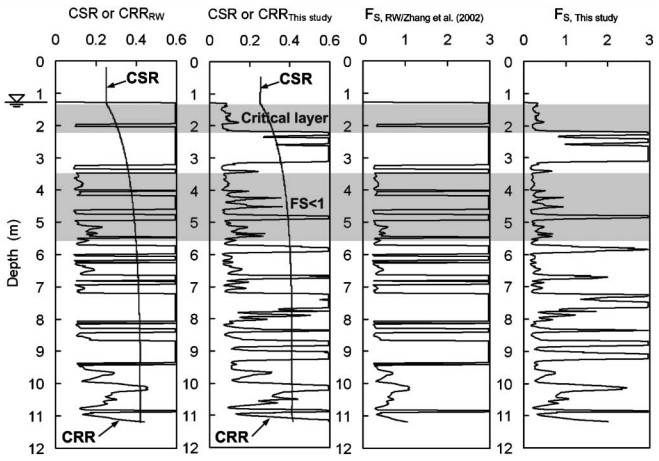

Fig. 14. Results of the analysis of Adapazari CPT-C4 using the Robertson and Wride (RW/Zhang) method and the proposed method (after Juang et al., 2008)

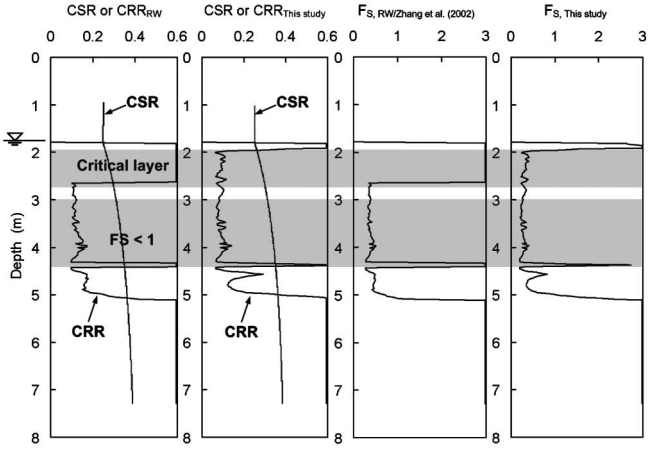

Fig. 16. Analytical results of CPT-B4 using the Robertson and Wride (RW/Zhang) method and the proposed CPTu method

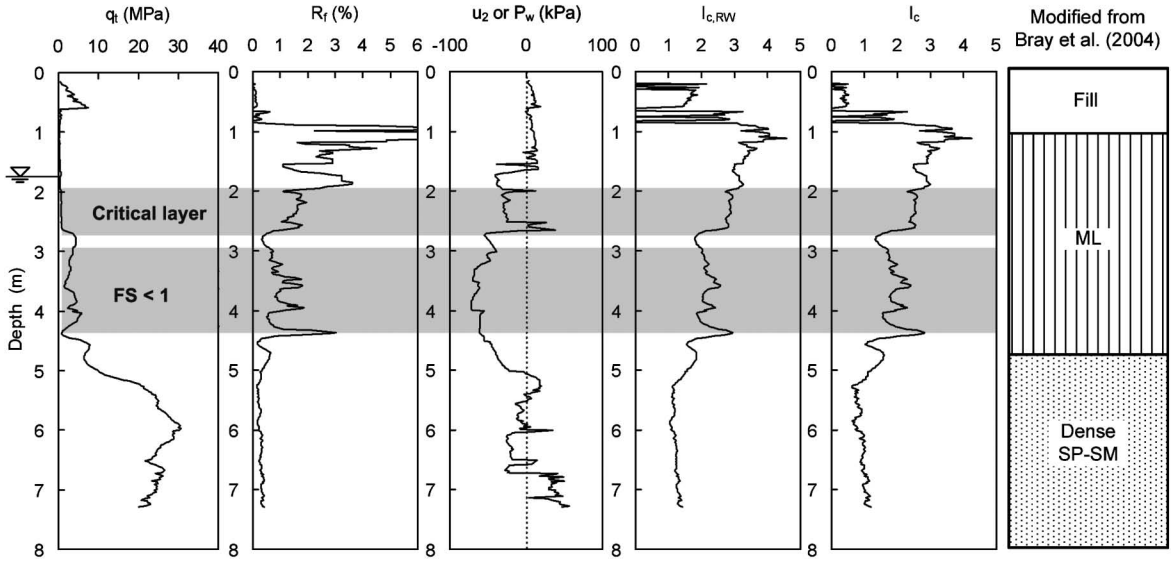

Fig. 15. CPTu sounding profiles and soil classification at location CPT-B4 in Adapazari

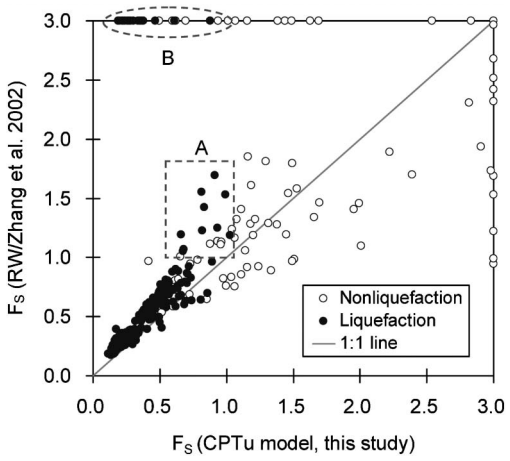

Fig. 17. Comparison of the F_S values computed with the two methods; liquefied cases in Zones A and B are more accurately predicted by the CPTu model

case at CPT-B4. The proposed method is shown again able to produce results that agree well with field observations. In the critical layer, the proposed method yields F_S much less than 1, whereas the Robertson and Wride method suggests that the soils are ''too clay-rich to liquefy.''

As a final comparison, Fig. 17 shows the factor of safety (F_S) computed with the RW/Zhang method (i.e., the Robertson and Wride method as updated in Zhang et al., 2002) and those computed with the proposed CPTu model. The data used in this analysis are those shown in Fig. 1. It is noted that for graphing purpose, the F_S values are set to 3 if the computed values are greater than 3. When the RW/Zhang method is employed, if a soil is judged to be too clay-rich to liquefy ($I_{c,RW} > 2.64$), its F_S value is artificially set to 3. As shown in Fig. 17, for most cases, the F_S values computed with the two methods are quite comparable. For some liquefied cases, shown in zones A and B in Fig. 17, the RW/Zhang method yields $F_S > 1$ (zone A) or $F_S \gg 1$ (zone B; cases that were judged to be too clay-rich to liquefy by the $I_{c,RW} > 2.64$ criterion of the RW/Zhang method), while the proposed CPTu model yields $F_S < 1$, suggesting that the proposed CPTu model yields more reasonable results in these cases. However, a few non-liquefied cases in zone B would have been incorrectly identified ($F_S < 1$) using the proposed model. Overall, the proposed CPTu model is seen as an improvement over the existing CPT-based methods.

SUMMARY AND CONCLUSIONS

A CPTu-based method for evaluating liquefaction potential of soils is presented which incorporates excess porewater pressure ratio (B_q) in the formulation of soil behavior type index (I_c), as defined by Jefferies and Davies (1993) and Jefferies and Been (2006). The developed CRR model must be used with the CSR model developed by Idriss and Boulanger (2006), as the latter is an integral part of the calibration process in developing the proposed CRR model. The model described here is more applicable to a *wider range* of geomaterials, including soils that were once considered ''too clay-rich to liquefy'' using the existing method. Thus, the results of the analysis using the proposed CPTu-based method will enable a more meaningful modeling of liquefaction effect within the framework of the Liquefaction Potential Index (LPI). In fact, calibration of the LPI framework that is developed based on the proposed CPTu model has been performed and satisfactory results have been reported (Juang et al., 2008).

The proposed CRR model is a function of two derived variables, q_{t1N} and I_c (as per Eqs. (2) and (3), respectively). Thus, the characteristics of the model can easily be depicted in 3-D graphs, in which its ability to delineate liquefied cases from non-liquefied cases is clearly shown. When data points of case histories are properly grouped, 2-D graphs can also delineate liquefied cases from non-liquefied cases. Examination of these 2-D graphs reveals that for soils with higher q_{t1N} (and thus lower I_c), the variable q_{t1N} has a much greater influence on liquefaction resistance than does the variable I_c. However, for soils with high I_c and low q_{t1N}, the variable I_c has a much greater influence on liquefaction resistance than the variable q_{t1N}. Thus, the traditional approach of using 2-D graphs of CSR versus q_{t1N} to examine the performance of a simplified CRR model has limitations. Therefore, the advantage of the proposed model in delineating liquefied cases from non-liquefied cases using 3-D graphs is clearly demonstrated.

The effect of the excess pore pressure ratio B_q is examined in this study. Neglecting B_q in the determination of I_c can lead to either an underestimation or overestimation of CRR, depending upon whether B_q is a positive or negative value. The trends of the effect of B_q on the calculated CRR are clearly observed. For ''silt mixture'' (clayey silt to silty clay) where the liquefaction resistance was previously ill-defined, a strong effect of B_q on the calculated CRR is clearly demonstrated.

The results of the analysis of cases from critical layers at selected ground failure sites in Adapazari using the proposed CPTu-based method agreed well with field observations in the 1999 Kocaeli earthquake. The results showed that those liquefied cases previously identified as ''too clay rich to liquefy'' based on the existing CPT-based methods can be correctly ''predicted'' using the proposed model.

The proposed CPTu model is shown to be comparable to the existing CPT-based methods such as the Robertson and Wride method in most of the cases examined. In some liquefied cases, particularly those that were judged to be too clay-rich to liquefied by the $I_{c,RW} > 2.64$ criterion, the proposed CPTu model is shown to be able to improve upon the Robertson and Wride method. Finally, it should be emphasized that the proposed CPTu model is not entirely new; it is built on the foundation of the previous work by many investigators.

ACKNOWLEDGMENTS

The results presented in this paper are a summary of research supported by the U.S. Geological Survey (USGS), Department of the Interior under USGS award number 07HQGR0053. The views and conclusions contained in this paper are those of the writers and therefore should not be interpreted as necessarily representing the official policies, expressed or implied, of the U.S. Government. The writers also wish to thank Mike Jefferies and Rodolfo Sancio of Golder Associates for their insights and helpful discussions on CPT measurements and effects of porewater pressure ratio.

NOTATION

q_c = raw cone tip resistance

q_t = cone tip resistance corrected for porewater pressure

f_s = sleeve friction

R_f = friction ratio = $f_s/q_t \cdot 100\%$

$u_2 = P_w$ = porewater pressure

B_q = excess porewater pressure ratio = $\dfrac{u_2 - u_o}{q_t - \sigma_{vo}}$

u_0 = hydrostatic water pressure

σ_{vo} = total vertical (overburden) stress

$Q_t = \dfrac{q_t - \sigma_{vo}}{\sigma'_{vo}}$ = normalized form of cone tip resistance

σ'_{vo} = effective vertical (overburden) stress

F = normalized sleeve friction = $\dfrac{f_s}{q_t - \sigma_{vo}} \times 100\%$

$I_{c,RW}$ = soil behavior type index defined by Robertson and Wride (1998)

$= \sqrt{(3.47 - \log_{10} Q_t)^2 + (\log_{10} F + 1.22)^2}$

I_c = soil behavior type index adopted in this paper (Eq. (3))

$= \sqrt{[3 - \log_{10}\{Q_t(1 - B_q) + 1\}]^2 + [1.5 + 1.3(\log_{10} F)]^2}$

q_{c1N} = stressed-adjusted cone tip resistance defined by Robertson and Wride (1998); obtained through an iterative process involving updating of a stress exponent, and

q_{t1N} = stressed-adjusted cone tip resistance defined by Idriss and Boulanger (2006) and adopted in this paper (Eq. (2)).

REFERENCES

1) Agrawal, G., Chameau, J. L. and Bourdeau, P. L. (1995): Assessing the liquefaction susceptibility at a site based on information from penetration testing, Chapter 9, *Artificial Neural Networks for Civil Engineers—Fundamentals and Applications*, ASCE Monograph, New York.

2) Boulanger, R. W. and Idriss, I. M. (2004): State normalization of penetration resistances and the effect of overburden stress on liquefaction resistance, *Proc. 11th SDEE and 3rd ICEGE*, Berkeley, California, 484–491.

3) Bray, J. D., Sancio, R. B., Durgunolu, T., Onalp, A., Youd, T. L., Stewart, J. P., Seed, R. B., Cetin, O. K., Bol, E., Baturay, M. B., Christensen, C. and Karadayilar, T. (2004): Subsurface characterization at ground failure sites in Adapazari, Turkey, *J. Geotech. and Geoenvir. Engrg.*, ASCE, **130**(7), 673–685.

4) Bray, J. D. and Sancio, R. B. (2006): Assessment of the liquefaction susceptibility of fine-grained soils, *J. Geotech. and Geoenvir. Engrg.*, ASCE, **132**(9), 1165–1177.

5) Bray, J. D., Sancio, R. B., Durgunolu, T., Onalp, A., Youd, T. L., Stewart, J. P., Seed, R. B., Cetin, O. K., Bol, E., Baturay, M. B., Christensen, C. and Karadayilar, T. (2006): Closure to subsurface characterization at ground failure sites in Adapazari, Turkey, *J. Geotech. and Geoenvir. Engrg.*, ASCE, **132**(4), 541–547.

6) Carraro, J. A. H., Bandini, P. and Salgado, R. (2003): Liquefaction resistance of clean and non-plastic silty sands based on cone penetration resistance, *J. Geotech. and Geoenvir. Engrg.*, ASCE, **129**(11), 965–976.

7) Cetin, K. O., Seed, R. B., Kiureghian, A. D., Tokimatsu, K., Harder, L. F., Jr., Kayen, R. E. and Moss, R. E. S. (2004): Standard penetration test-based probabilistic and deterministic assessment of seismic soil liquefaction potential, *J. Geotech. and Geoenvir. Engrg.*, ASCE, **130**(12), 1314–1340.

8) Demuth, H. and Beale, M. (2002): *Matlab Neural Network Toolbox, User's Guide*, The MathWorks, Inc., Natick, Mass.

9) Goh, A. T. C. (1994): Seismic liquefaction potential assessed by neural networks, *J. Geotech. and Geoenvir. Engrg.*, ASCE, **120**(9), 1467–1480.

10) Goh, A. T. C. (1996): Neural network modeling of CPT seismic liquefaction data, *J. Geotech. and Geoenvir. Engrg.*, ASCE, **122**(1), 70–73.

11) Gratchev, I. B., Sassa, K. and Fukuoka, H. (2006): How reliable is the plasticity index for estimating the liquefaction potential of clayey sands, *J. Geotech. and Geoenvir. Engrg.*, ASCE, **132**(1), 124–127.

12) Guo, T. and Prakash, S. (1999): Liquefaction of silts and silt-clay mixtures, *J. Geotech. and Geoenvir. Engrg.*, ASCE, **125**(8), 706–710.

13) Hagan, M. T. and Menhaj, M. (1994): Training feedforward networks with the Marquardt algorithm, *IEEE Transactions on Neural Networks*, **5**(6), 989–993.

14) Idriss, I. M. and Boulanger, R. W. (2004): Semi-empirical procedures for evaluating liquefaction potential during earthquakes, *Proc. 3rd International Conf. on Earthquake Geotechnical Engineering* (ICEGE), Berkeley, CA, 32–56.

15) Idriss, I. M. and Boulanger, R. W. (2006): Semi-empirical procedures for evaluating liquefaction potential during earthquakes, *Soil Dynamics and Earthquake Engineering*, **26**, 115–130.

16) Ishihara, K. (1993): Liquefaction and flow failure during earthquakes, *Geotechnique*, **43**(3), 351–415.

17) Iwasaki, T., Arakawa, T. and Tokida, K. (1982): Simplified procedures for assessing soil liquefaction during earthquakes, *Proc. Conf. on Soil Dynamics and Earthquake Engineering*, Southampton, UK, 925–939.

18) Jefferies, M. G. and Davies, M. P. (1993): Use of CPTu to estimate equivalent SPT N_{60}, *Geotechnical Testing Journal*, **16**(4), American Society for Testing and Materials, 458–468.

19) Jefferies, M. G. and Been, K. (2006): *Soil Liquefaction—A Critical State Approach*, Taylor & Francis Group, New York, NY.

20) Juang, C. H., Chen, C. J. and Tien, Y. M. (1999a): Appraising CPT-based liquefaction resistance evaluation methods—artificial neural network approach, *Canadian Geotechnical Journal*, **36**(3), 443–454.

21) Juang, C. H., Rosowsky, D. V. and Tang, W. H. (1999b): Reliability-based method for assessing liquefaction potential of sandy soils, *J. Geotech. and Geoenvir. Engrg.*, **125**(8), 684–689.

22) Juang, C. H., Chen, C. J., Tang, W. H. and Rosowsky, D. V. (2000): CPT-based liquefaction analysis, Part 1: Determination of limit state function, *Geotechnique*, **50**(5), 583–592.

23) Juang, C. H., Jiang, T. and Andrus, R. D. (2002): Assessing probability-based methods for liquefaction evaluation, *J. Geotech. and Geoenvir. Engrg.*, ASCE, **128**(7), 580–589.

24) Juang, C. H., Yuan, H., Lee, D. H. and Lin, P. S. (2003): Simplified CPT-based method for evaluating liquefaction potential of

soils, *J. Geotech. and Geoenvir. Engrg.*, ASCE, **129**(1), 66–80.
25) Juang, C. H., Fang, S. Y. and Khor, E. H. (2006): First order reliability method for probabilistic liquefaction triggering analysis using CPT, *J. Geotech. and Geoenvir. Engrg.*, **132**(3), 337–350.
26) Juang, C. H., Liu, C. N., Chen, C. H., Hwang, J. H. and Lu, C. C. (2008): Calibration of liquefaction potential index: A re-visit focusing on a new CPTU model, *Engineering Geology*, 2008, **102**(1–2), 19–30.
27) Kim, Y. S. and Kim, B. T. (2006): Use of artificial neural networks in the prediction of liquefaction resistance of sands, *J. Geotech. and Geoenvir. Engrg.*, **132**(11), 1502–1504.
28) Kishida, H. (1969): Characteristics of liquefied sands during Mino-Owari, Tohnankai and Fukui earthquakes, *Soils and Foundations*, **9**(1), 75–92.
29) Ku, C. S., Lee, D. H. and Wu, J. H. (2004): Evaluation of soil liquefaction in the Chi-Chi, Taiwan earthquake using CPT, *Soil Dynamics and Earthquake Engineering*, **24**, 659–673.
30) Lai, S. Y., Hsu, S. C. and Hsieh, M. J. (2004): Discriminant model for evaluating soil liquefaction potential using cone penetration test data, *J. Geotech. and Geoenvir. Engrg.*, ASCE, **130**(12), 1271–1282.
31) Li, D. K., Juang, C. H. and Andrus, R. D. (2006): Liquefaction potential index: a critical assessment, *J. GeoEngineering*, Taiwanese Geotechnical Society, **1**(1), 11–24.
32) Li, D. K., Juang, C. H., Andrus, R. D. and Camp, W. M. (2007): Index properties-based criteria for liequefaction susceptibility of clayey soils: a critical assessment, *J. Geotech. and Geoenvir. Engrg.*, ASCE, **133**(1), 110–115.
33) MathWork, Inc. (2002): *Matlab Version 6.5*, Natick, MA.
34) Mitchell, J. K. and Tseng, D. J. (1990): Assessment of liquefaction potential by cone penetration resistance, *Proc. H. Bolton Seed Memorial Symposium* (ed. by J. M. Duncan), Vancouver, B.C., **2**, 335–350.
35) Moss, R. E. S., Seed, R. B., Kayen, R. E., Stewart, J. P., Der Kiureghian, A. and Cetin, K. O. (2006): CPT-based probabilistic and deterministic assessment of in situ seismic soil liquefaction potential, *J. Geotech. and Geoenvir. Engrg.*, ASCE, **132**(8), 1032–1051.
36) Olsen, R. S. (1997): Cyclic liquefaction based on the cone penetrometer test, *Proc. the NCEER Workshop on Evaluation of Liquefaction Resistance of Soils*, Technical Report NCEER–97–0022 (eds. by T. L. Youd and I. M. Idriss), National Center for Earthquake Engineering Research, State University of New York at Buffalo, Buffalo, NY, 225–276.
37) PEER web site (2007): Soils and liquefaction data on 1999 Kocaeli, Turkey Earthquake, http://peer.berkeley.edu/publications/turkey/adapazari/index.html.
38) Perlea, V. G., Koester, J. P. and Prakash, S. (1999): How liquefiable are cohesive soils, *Proc. 2nd Int. Conf. on Earthquake Geotechnical Engineering*, Lisbon, Portugal, 611–618.
39) Robertson, P. K. and Campanella, R. G. (1985): Liquefaction potential of sand using the CPT, *J. Geotech. Engrg.*, ASCE, **111**(3), 384–403.
40) Robertson, P. K. (1990): Soil classification using the cone penetration test, *Canadian Geotechnical Journal*, **27**(1), 151–158.
41) Robertson, P. K. and Wride, C. E. (1998): Evaluating cyclic liquefaction potential using the cone penetration test, *Canadian Geotechnical Journal*, **35**(3), 442–459.
42) Rumelhart, D. E., Hinton, G. E. and Williams, R. J. (1986): Learning internal representations by error propagation, Parallel Distributed Processing: Foundations, **1** (eds. by D. E. Rumelhart and J. L. McClelland), MIT Press, Combridge, Mass, 318–362.
43) Seed, H. B. and Idriss, I. M. (1971): Simplified procedure for evaluating soil liquefaction potential, *J. Soil Mechanics and Foundation Div.*, ASCE, **97** (SM9), 1249–1273.
44) Seed, H. B., Tokimatsu, K., Harder, L. F. and Chung, R. (1985): Influence of SPT procedures in soil liquefaction resistance evaluations, *J. Geotechnical Engrg.*, ASCE, **111**(12), 1425–1445.
45) Seed, H. B. and de Alba, P. (1986): Use of SPT and CPT tests for evaluating liquefaction resistance of sands, *Use of In Situ Testing in Geotechnical Engineering*, Geotechnical Special Publication No. 6, ASCE, New York, 281–302.
46) Shuttle, D. A. and Cunning, J. (2007): Liquefaction potential of silts from CPTu, *Canadian Geotechnical Journal*, **44**(1), 1–19.
47) Stark, T. D. and Olson, S. M. (1995): Liquefaction resistance using CPT and field case histories, *J. Geotech. and Geoenvir. Engrg.*, ASCE, **121**(GT 12), 856–869.
48) Suzuki, Y., Koyamada, K., Tokimatsu, K., Taya, Y. and Kubota, Y. (1995): Empirical correlation of soil liquefaction based on cone penetration test, *Earthquake Geotechnical Engineering* (ed. by K. Ishihara), Balkema, Rotterdam, The Netherlands, 369–374.
49) Thevanayagam, S., Fiorillo, M. and Liang, J. (2000): Effect of nonplastic fines on undrained cyclic strength of silty sands, *Soil Dynamics and Liquefaction 2000* (eds. by Pak, R. Y. S. and Yamamura, J.), Geotechnical Special Publication No. 107, ASCE, Reston, VA, 77–91.
50) Tohno, I. and Yasuda, S. (1981): Liquefaction of the ground during the 1978 Miyagiken-Oki earthquake, *Soils and Foundations*, **21**(3), 18–34.
51) Toprak, S. and Holzer, T. L. (2003): Liquefaction potential index: field assessment, *J. Geotech. and Geoenvir. Engrg.*, ASCE, **129**(4), 315–322.
52) Youd, T. L., Idriss, I. M., Andrus, R. D., Arango, I., Castro, G., Christian, J. T., Dobry, R., Liam Finn, W. D., Harder, L. F., Jr., Hynes, M. E., Ishihara, K., Koester, J. P., Laio, S. S. C., Marcuson, W. F., III, Martin, G. R., Mitchell, J. K., Moriwaki, Y., Power, M. S., Robertson, P. K., Seed, R. B. and Stokoe, K. H., II. (2001): Liquefaction resistance of soils: summary report from the 1996 NCEER and 1998 NCEER/NSF workshops on evaluation of liquefaction resistance of soils, *J. Geotech. and Geoenvir. Engrg.*, **127**(10), 817–833.
53) Zhang, G., Robertson, P. K. and Brachman, R. W. I. (2002): Estimating liquefaction-induced ground settlements from CPT for level ground, *Canadian Geotechnical Journal*, **39**(5), 1168–1180.